International Journal of Advanced Engineering Research and Science (IJAERS)
Peer-Reviewed Journal
ISSN: 2349-6495(P) | 2456-1908(O)
Vol-12, Issue-8; Aug, 2025
Journal Home Page Available: https://ijaers.com/
Article DOI: https://dx.doi.org/10.22161/ijaers.128.5

Numerical Simulation and Analysis of Gas-Liquid Two-Phase Flow in a Venturi Tube

Yong-Sen Huang, Yan-Zuo Chang*, Qi-Hong Tang, Guo-Xing Yang, Liu-Yi Yu, Ruo-Yu Yang, Jin-Ping Chen, Ying-Xiang Mo

Energy and Power Engineering, Guangdong University of Petrochem Technology (GDUPT), Maoming525000, China
*Corresponding author:

Received: 25 Jul 2025,

Received in revised form: 23 Aug 2025,

Accepted: 27 Aug 2025,

Available online: 31 Aug 2025

***Keywords*— Venturi tube, Fluent fluid analysis, gas-liquid two-phase flow.**

***Abstract*—** *The Venturi tube, a widely used cavitation-generating device in the petroleum and chemical industries, is valued for its simple structure and safe stability. During cavitation-induced gas-liquid two-phase flow, collapsing bubble clusters release high temperature and pressure energy with associated effects. This study uses Fluent to investigate the Venturi tube's internal flow field characteristics. By comparing pressure contours, velocity contours, and gas phase distributions under varying inlet-outlet pressure ratios, throat length-to-diameter ratios, and diffusion angles, it analyzes cavitation flow evolution. Results show: for a fixed-structure Venturi with constant outlet pressure, stronger cavitation effects occur with higher inlet pressure, larger throat length-to-diameter ratios, and smaller diffusion angles. These findings clarify internal flow patterns and the influence of hydraulic and structural parameters on cavitation intensity.*

I. INTRODUCTION

The Venturi tube is typically made of cast iron or steel. In its cross-sectional structure, the pipe section is larger at both ends than in the middle, with the smallest cross-sectional area being the throat. When fluid flows through the Venturi tube, due to the reduction of the pipe's cross-sectional area, the flow velocity increases, and the pressure correspondingly decreases, so the flow velocity is the greatest and the pressure is the lowest at the throat [1]. By leveraging the relationship between pressure difference and velocity in a horizontal state, the Venturi tube can be used to measure fluid velocity or flow rate, that is, the flow and velocity can be inferred from the pressure difference generated after the fluid flows through.

According to Bernoulli's law, in a steady and continuous flow field, the pressure must decrease where the flow velocity increases [2]. The Venturi tube operates on this principle: minimal pressure loss, no fouling, wide range, and capable of measuring large flows. It has now been widely applied in automotive carburetors, electrostatic precipitators, vacuum cleaners, coolers, dryers, and so on [3]. Based on these advantages, academic research on the Venturi tube continues to deepen. In 2013, Wang Changbin simulated the characteristics of cavitation gas-liquid two-phase flow in the Venturi tube through fluid mechanics simulation software and concluded that when other conditions remain unchanged, reducing the throat diameter or increasing the inlet pressure both increase the throat velocity and decrease the local static pressure, thereby enhancing cavitation; extending the length of the diffuser section delays the recovery of the adverse pressure gradient, prolonging the cavitation bubble growth and collapse process, and enhancing the cavitation gas-liquid two-phase flow effect. This conclusion has great reference value for actual engineering projects [4]. In 2014, Capocelli et al. proposed a comprehensive modeling method for estimating reactor performance, combining cavity dynamics with Bernoulli-type macroscopic flow calculations to estimate turbulent fluctuations, which provides a more effective framework for developing a general prediction model for cavitation reactors [5]. In 2016, Xianlin Li and Biao Huang

studied the influence of orifice plate geometric parameters on cavitation in the Venturi tube and further explored the free radicals generated by cavitation effects, and the results showed that the throat diameter of the Venturi tube has a greater impact on cavitation effects than the throat length; the evolution intensity of cavitation-induced gas-liquid two-phase flow inside the Venturi tube is of great significance to the stable operation and structural integrity of engineering facilities [6]. In 2017, Long et al. and Brinkhorst et al. achieved high-speed visualization of cavitation onset and growth in Venturi tube devices through experimental research, clearly describing the development of cavitation and its impact on overall equipment operation from the perspectives of flow rate and pressure [7-8]. The Venturi cavitation reactor has become an experimental hotspot, attracting attention for its significant efficiency in wastewater treatment and various process enhancements.

In summary, while basic research on Venturi tubes has matured, the complex dynamics of cavitation-induced gas-liquid two-phase flow under special working conditions still require deeper exploration. This study uses Fluent to perform three-dimensional numerical simulations of cavitation cloud evolution, systematically adjusting key parameters like pressure ratios, diffusion angles, and throat length-to-diameter ratios. By extracting critical flow field features (such as cavitation volume fraction and pressure fluctuation patterns) and quantifying how structural design and operating conditions interact, the research provides valuable insights for both cavitation inhibition and energy utilization. These findings will directly support the optimized design of Venturi tubes, enhancing their operational economy and long-term reliability in practical applications.

II. RESEARCH METHODS

2.1 Establishment of the Physical Model and Parameter Selection

The specific structure of the Venturi tube studied in this paper is shown in Figure 1. Based on the actual working parameters of the Venturi tube, the inlet pressure is 0.3–0.6 MPa, and the outlet pressure is 0.1 MPa. The model defines the inlet diameter of the contraction section as D = 50 mm, the throat diameter as d = 10 mm, the throat length as L = 10 mm, the contraction angle α = 22.5°, and the diffusion angle β = 6° [9].

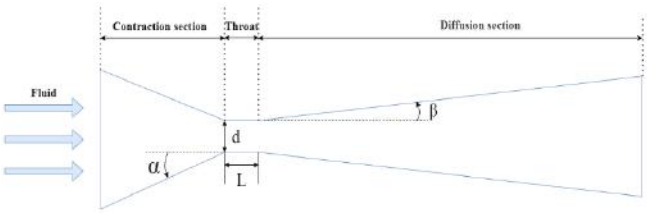

Fig.1 Venturi tube physical model

2.2 Establishment of the Mathematical Model

Liu Houlin et al. compared the application of three different models in cavitation flow calculations of centrifugal pumps and found that if the Zwart cavitation model is used for simulating the flow coefficient, the simulation results are closer to the experimental values [10]. The final form of the cavitation model proposed by Zwart-Gerber-Belamri is as follows:

If $P \leq P_V$

$$R_e = F_{vap}\frac{3\alpha_{nuc}(1-\alpha_v)\rho_v}{R_B}\sqrt{\frac{2}{3}\frac{P_V-P}{\rho_1}} \quad (1)$$

If $P > P_V$

$$R_C = F_{cond}\frac{3\alpha_v\rho_V}{R_B}\sqrt{\frac{2}{3}\frac{P-P_V}{\rho_1}} \quad (2)$$

where: R_e is the vaporization rate, R_B is the bubble radius, taken as R_B=$10^{-6}m$; α_{nuc} is the nucleation partial volume fraction, taken as α_{nuc}=5×; F_{vap} is the empirical correction coefficient for the evaporation term, taken as F_{vap}=50; F_{cond} is the empirical correction coefficient for the condensation term, taken as F_{cond} =0.001; P_V is the critical cavitation pressure; P is the flow field pressure; ρ1 is the liquid phase density; R_C is the condensation rate; ρ_1 is the gas phase density.

When fluid flow passes through the wall surface, there is a viscous force that causes excessive gradient changes. In this region, the Reynolds number of turbulence becomes smaller, and a laminar effect will occur. The wall function is a set of semi-empirical formulas that derive the velocity physical quantities in this region [11]. The momentum equation for the wall function is:

$$U^* = \frac{1}{K_C}ln(E_C y^*) \quad (3)$$

U^* is the dimensionless velocity

$$U^* = \frac{U_P C_\mu^{\frac{1}{4}} K_P^{\frac{1}{2}}}{\frac{t_W}{\rho}} \quad (4)$$

y^* is the dimensionless distance from the wall

$$y^* = \frac{\rho C_\mu^{\frac{1}{4}} K_P^{\frac{1}{2}} y_P}{\mu} \quad (5)$$

where: K_C is the von Kármán constant, usually taken as 0.4187; E_C is the empirical constant, taken as 9.793; U_P is the average velocity at the wall surface node P; K_p is the turbulent kinetic energy near the wall surface node P; y_P is the distance from point P to the wall surface.

III. NUMERICAL SIMULATION

After obtaining the geometric model of the Venturi tube, mesh generation is also a key step: considering the abrupt pressure changes and complex flow field caused by cavitation, the computational dimension will increase exponentially with mesh refinement. Therefore, a non-structured mesh that is highly adaptable to arbitrary boundaries and easy to locally refine is adopted: the overall mesh is divided using the Fluent non-structured mesh, and the mesh quantity is refined in key areas such as the throat and diffuser section to ensure accuracy, while the contraction section is moderately sparse to reduce computational load and accelerate convergence, as shown in Figure 2 [12].

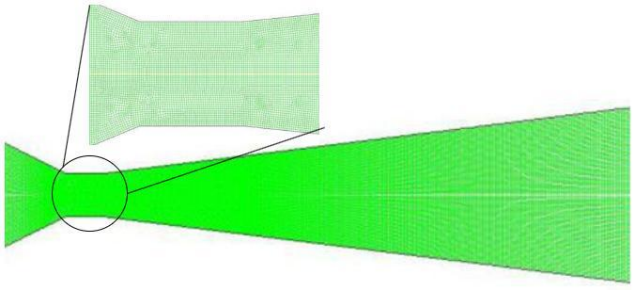

Fig.2 Venturi tube mesh generation

To simplify the model, the following assumptions are made for the control equations: the medium is steady-state, single-phase fluid with constant viscosity, density, and diffusion coefficient; there is no chemical reaction between the cavitation gas-liquid two-phase flow, and gravity is neglected. Based on these assumptions, the CFD software FLUENT is used to conduct numerical simulations of the flow field inside the Venturi tube.

3.1 Investigation of the Influence of Different Inlet Pressures on the Venturi Tube

Under other conditions remaining unchanged, the inlet pressure is set to 0.3 MPa, 0.4 MPa, 0.5 MPa, and 0.6 MPa respectively, to simulate and analyze the fluid velocity, pressure, and gas phase distribution inside the Venturi tube under different inlet pressures. The resulting diagrams are as follows.

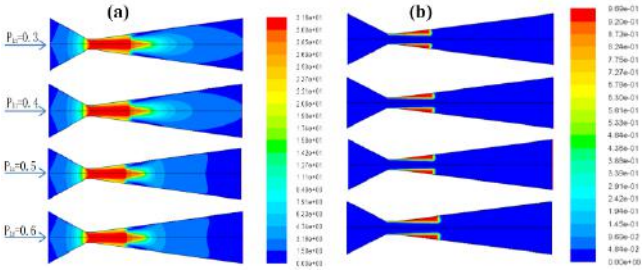

Fig.3 Velocity (a) and gas phase distribution (b) changes in the Venturi tube under different inlet pressures

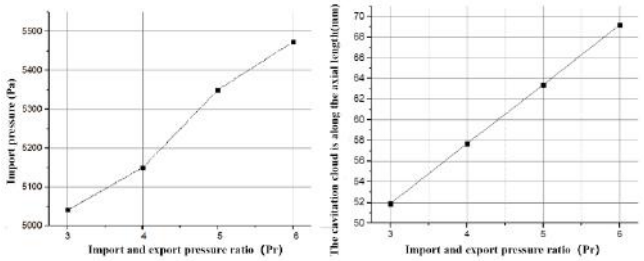

Fig.4 Pressure and cavitation cloud distribution along the axial length of the Venturi tube under different inlet and outlet pressure ratios

From the velocity contour in Figure 3(a), it can be seen that when the inlet and outlet pressure ratio is 6, the fluid velocity reaches a maximum of 31.6 m/s at the throat, and the maximum velocity increases with higher inlet pressure. The larger the inlet pressure, the larger the high-speed region at the throat. As the contraction section is entirely liquid, from the gas phase distribution in Figure 3(b), it can be observed that cavitation gas-liquid two-phase flow bubbles are generated at the junction of the contraction section and the front end of the throat, and more bubbles are produced at this junction than at the front end of the throat. After the front half of the diffuser section, the bubble diameter reduces to zero.

From Figure 4, it can be seen that under different inlet pressure conditions, the minimum pressure at the throat increases with the increase in inlet pressure, and the overall change is not very uniform. From the cavitation cloud diagram, it can be observed that as the inlet and outlet pressure ratio increases, the growth rate of the cavitation cloud length increases linearly.

3.2 Investigation of the Influence of Different Diffusion Angles on the Venturi Tube

With the throat length L = 10 mm, the contraction angle set to 22.5°, and the inlet pressure at 0.4 MPa, the diffusion angle is set to 6°, 9°, 12°, and 15° respectively. The simulation analysis of the fluid velocity, pressure, and gas

phase distribution inside the Venturi tube under different inlet pressures is shown in Figure 5.

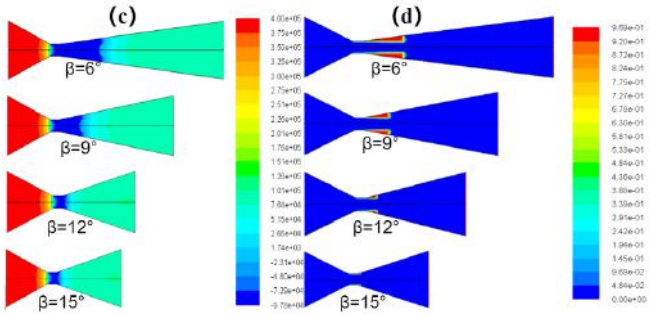

Fig.5 Pressure (c) and gas phase distribution (d) inside the Venturi tube under different diffusion angles

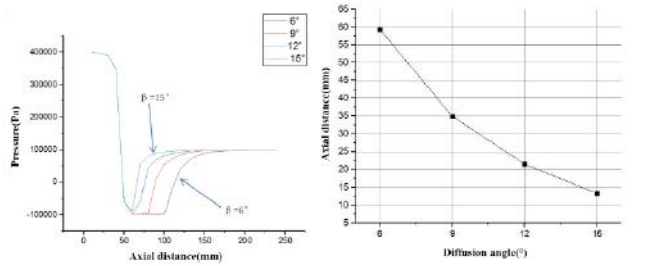

Fig.6 Axial pressure distribution and cavitation cloud length of the Venturi tube under different diffusion angles

As the diffusion angle of the Venturi tube increases, from the pressure contour (c), it can be seen that the low-pressure region decreases with the increase in the diffusion angle. Combined with Figure 3(a), it can be observed that the larger the diffusion angle, the faster the water flow velocity decays, the faster the pressure recovery in the diffuser section, and the smaller the low-pressure region. From the gas phase distribution diagram (d) of the Venturi tube, it can be seen that as the diffusion angle increases, the bubble range gradually decreases, and the starting point of generation gradually moves backward. That is, the smaller the diffusion angle of the Venturi tube, the greater the axial distance of the cavitation cloud length. Because bubbles can move further with the higher-velocity water flow and delay collapse, the cavitation gas-liquid two-phase flow bubble cloud region decreases with the increase in the diffusion angle.

From the axial pressure diagram of the Venturi tube in Figure 6, it can be seen that the diffusion angle has the greatest impact on the throat, and the larger the diffusion angle, the faster the pressure change. From the cavitation cloud length diagram, it can be more intuitively seen that as the diffusion angle increases, the axial distance of the cavitation cloud length decreases.

3.3 Investigation of the Influence of Different Throat Lengths on the Venturi Tube

The throat lengths are 0 mm, 10 mm, 20 mm, and 30 mm respectively, with other conditions remaining unchanged, the inlet pressure is 0.4 MPa, and the outlet pressure is 0.1 MPa.

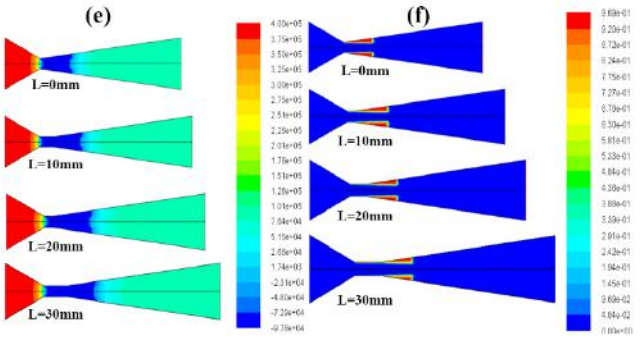

Fig.7 Pressure (e) and gas phase distribution (f) inside the Venturi tube under different throat lengths

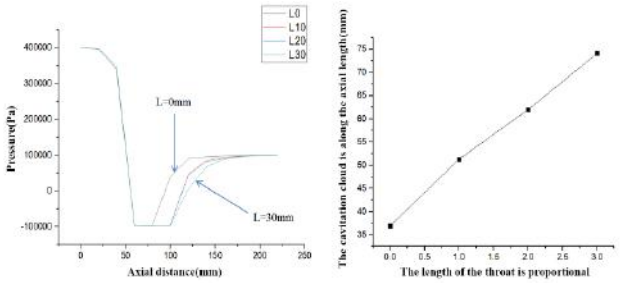

Fig.8 Axial pressure variation curve and cavitation cloud axial length of the Venturi tube under different throat lengths

The pressure contour (e) in Figure 7 reflects that as the throat length increases, the pressure recovery slows down, meaning that increasing the throat length within the Venturi tube delays pressure recovery. The gas phase distribution diagram (f) shows that bubbles are generated at both the throat inlet and outlet, with fewer bubbles at the throat inlet and larger bubble areas at the outlet.

From the axial pressure diagram in Figure 8, it can be seen that different throat lengths mainly affect the pressure at the end of the throat. When the throat length increases from 0–10 mm, the pressure changes rapidly, and then from 10–20 mm, the changes slow down. Overall, as the length increases, the rate of change tends to flatten. The cavitation cloud length diagram shows that the cavitation gas-liquid two-phase flow cavitation cloud length within the Venturi tube increases with the increase in the length-to-diameter ratio.

IV. CONCLUSION

This study employs the Fluent software to conduct numerical simulations of the fluid inside the Venturi tube, analyzing the basic characteristics of the flow field from three aspects: pressure, velocity, and phase diagrams. Using the numerical model, the generation and variation trends of cavitation gas-liquid two-phase flow under different structural designs and working conditions were analyzed. Through numerical simulation analysis, the following conclusions were drawn:

For the same Venturi tube with constant structural size and stable outlet pressure, as the inlet pressure increases, the area of the cavitation gas-liquid two-phase flow cloud also increases. Appropriately increasing the inlet and outlet pressure ratio is beneficial for enhancing the cavitation gas-liquid two-phase flow effect. The change in the throat length-to-diameter ratio (i.e., the ratio of throat length to throat diameter L/d) has little impact on the initial point of cavitation gas-liquid two-phase flow generation, but it helps to delay pressure recovery within the tube, allowing the cavitation cloud to develop better and collapse later. Under other conditions remaining the same, the cavitation gas-liquid two-phase flow cavitation cloud length within the Venturi tube increases with the increase in the length-to-diameter ratio L/d. Changes in the diffusion angle have a significant impact on the initiation and evolution of cavitation gas-liquid two-phase flow; a smaller diffusion angle is conducive to the generation and development of cavitation gas-liquid two-phase flow, causing cavitation to occur at lower pressures, advancing the starting point of cavitation, and subsequently providing more time and space for bubble generation and growth, with the final collapse region of the gas-liquid two-phase flow cavitation cloud moving backward.

Through the study of cavitation in the Venturi tube and combining the conclusions, in engineering fields such as wastewater treatment and food processing that require the enhancement and utilization of cavitation gas-liquid two-phase flow effects, we can strengthen the cavitation effect by increasing the inlet pressure, appropriately reducing the diffusion angle, and increasing the throat length-to-diameter ratio, thereby better applying the cavitation effect in industrial fields. In terms of reducing the damage caused by cavitation, such as in water conservancy projects, hydraulic machinery, and ships, we can weaken the cavitation effect by reducing the inlet pressure, appropriately increasing the diffusion angle, and decreasing the throat length-to-diameter ratio. In addition to these measures, reinforcing or adding wear-resistant coatings in areas prone to cavitation—where flow velocity increases sharply and pressure drops significantly—can also minimize the damage caused by cavitation gas-liquid two-phase flow effects.

ACKNOWLEDGEMENTS

This research was supported by "Guangdong Science and Technology Program", "Lagrangian Coherent Structure Analysis of Heat Sink for Heat Transfer". Analysis of Heat Sink for Heat Transfer Performance with Piezoelectric Fan. (NO. 2024A0505050022)", the Innovation Fund for Energy and Power Engineering named "Photovoltaic storage refrigeration clothing, (NO.20242C02)" from the School of Energy and Power Engineering, Guangdong University of Petrochemical Technology. Research on Intelligent Monitoring and Control Technology of Air Conditioning Noise Based on Quantitative Conjugate Gradient Method. Guangdong College Students' Innovation and Entrepreneurship Program in 2025, (Project No.: 25A015).

REFERENCES

[1] Ma, Y., Yan, Y. F., Zhang, A. Q., & Liu, P. (2022). Study on cavitation characteristics of a venturi throttle tube applied in nuclear power. *Low Temperature and Superconductivity*, 50(9), 65–72+100.

[2] Hu, Y., Liu, M. Y., & Liu, Z. H. (2022). Structural design and simulation analysis of venturi tube for ring pump foam system in fire trucks. *Special Purpose Vehicle*, (5), 42–44.

[3] Hai, Q., Chen, W. Z., & Yan, K. (2023). Numerical simulation of a new venturi cavitator and its cavitation characteristics. *Journal of Ship Mechanics*, 27(10), 1464–1474.

[4] Wang, C. B., Wang, M., et al. (2013). CFD simulation of hydrodynamic cavitation in venturi tubes. *Pipeline Technology and Equipment*, (1), 10–12.

[5] Capocelli, M., Musmarra, D., Prisciandaro, M., & Industriale, I. (2014). Chemical effect of hydrodynamic cavitation: Simulation and experimental comparison. *AIChE Journal*, 60(7), 2566–2572.

[6] Li, X. L., Huang, B., & Chen, T. R. (2016). Combined experimental and computational investigation of the cavitating flow in an orifice plate with special emphasis on surrogate-based optimization method. *Journal of Mechanical Science and Technology*, 31(1), 269–279.

[7] Long, X., Zhang, J., Wang, J., Xu, M., Lyu, Q., & Ji, B. (2017). Experimental investigation of the global cavitation dynamic behavior in a venturi tube with special emphasis on the cavity length variation. *International Journal of Multiphase Flow*, 89, 290–298.

[8] Brinkhorst, S., von Lavante, E., & Wendt, G. (2017). Experimental and numerical investigation of the cavitation-induced choked flow in a Herschel venturi-tube. *Flow Measurement and Instrumentation*, 54, 56–67.

[9] Taki, K., Hosseinzadeh Samani, B., Izadi, Z., Rostami, S., & Nazai, F. (2025). Non-thermal inactivation of *Escherichia coli* in milk using a Venturi tube reactor and liquid-phase

plasma: A parametric optimization study. *International Dairy Journal*, 167, 106269.

[10] Liu, H. L., Liu, D. X., Wang, Y., et al. (2012). Evaluation of three cavitation models in cavitating flow calculation of centrifugal pumps. *Transactions of the Chinese Society of Agricultural Engineering*, 28(16), 54–59.

[11] Wang, H. G., Pang, J. W., Song, Q. H., Li, H., Yang, X., & Deng, T. P. Numerical simulation study on enhancing hydrodynamic cavitation in venturi tubes. *Intelligent Computer and Applications*, 1–6. https://doi.org/10.202169/j.issn.2095-2163.24092901.

[12] Tang, Z. H., Dong, L. F., Wu, X., Xin, Y. P., & Xin, Y. B. (2021). Study on flow pressure drop characteristics of gas-liquid two-phase flow in venturi tube. *Shandong Chemical Industry*, 50(13), 169–171. https://doi.org/10.19319/j.cnki.issn.1008-021x.2021.13.069.